MITSUBISHI ELECTRIC RESEARCH LABORATORIES
http://www.merl.com

A High Efficiency 3.6-4.0 GHz Envelope-Tracking Power Amplifier Using GaN Soft-Switching Buck-Converter

Komatsuzaki, Y.; Lanfranco, S.; Komlonen, T.; Piirainen, O.; Tanskanen, J.; Sakata, S.; Ma, R.; Shinjo, S.; Yamanaka, K.; Asbeck, P.

TR2018-073 July 12, 2018

Abstract

We report a high efficiency sub-6GHz wideband Envelope-Tracking Power Amplifier (ET-PA) including a softswitching buck-converter and a wideband RF-PA, used in conjunction with a digital front end (DFE) environment for signal generation and predistortion. Both buck-converter and RF-PA were fabricated using an 0.15um GaN HEMT process. The DFE can generate the input signals for both buck-converter and RFPA, capture the output signal for feed-back and perform digital predistortion (DPD). The overall ET-PA achieves total efficiency of 39.5-46.7% and output power of 31.2-31.5dBm over 3.6- 4.0GHz with 20MHz LTE signals. With DPD, ACLR was below -45dBc with total efficiency reaching 47% at 3.6GHz. This, to the best of the authors knowledge, is the highest efficiency yet reported for an ET-PA at this carrier frequency.

IEEE International Microwave Symposium (IMS)

A High Efficiency 3.6-4.0 GHz Envelope-Tracking Power Amplifier Using GaN Soft-Switching Buck-Converter

Yuji Komatsuzaki[1,2], Sandro Lanfranco[3], Tapio Kolmonen[4], Olli Piirainen[4], Jarno K. Tanskanen[4], Shuichi Sakata[2], Rui Ma[5], Shintaro Shinjo[2], Koji Yamanaka[2], Peter Asbeck[1]

[1]University of California, San Diego, La Jolla, CA 92093, USA
[2]Mitsubishi Electric Corporation, Kamakura, Kanagawa, 247-8501, Japan
[3]NOKIA Bell Labs, Sunnyvale, CA 94086, USA
[4]NOKIA Bell Labs, Oulu 90620, Finland
[5]Mitsubishi Electric Research Laboratories, Cambridge, MA 02139, USA

***Abstract*— We report a high efficiency sub-6GHz wideband Envelope-Tracking Power Amplifier (ET-PA) including a soft-switching buck-converter and a wideband RF-PA, used in conjunction with a digital front end (DFE) environment for signal generation and predistortion. Both buck-converter and RF-PA were fabricated using an 0.15um GaN HEMT process. The DFE can generate the input signals for both buck-converter and RF-PA, capture the output signal for feed-back and perform digital predistortion (DPD). The overall ET-PA achieves total efficiency of 39.5-46.7% and output power of 31.2-31.5dBm over 3.6-4.0GHz with 20MHz LTE signals. With DPD, ACLR was below -45dBc with total efficiency reaching 47% at 3.6GHz. This, to the best of the authors' knowledge, is the highest efficiency yet reported for an ET-PA at this carrier frequency.**

***Index Terms*— GaN, Power Amplifier, PAE, Switching-Mode Power Amplifier, Envelope Tracking**

I. Introduction

Recently, advanced wireless communication systems apply high peak-to-average power ratio (PAPR) signals to cope with crowded spectrum and higher speed data demands. RF power amplifiers for base stations require high efficiency at a large back-off level (>6.5dB). Amplifier operation at frequencies above 3 GHz is increasingly important for 4G and 4.5G systems, and is a cornerstone of emerging sub-6GHz 5G systems. The amplifiers must accommodate a wide range of carrier frequencies (potentially up to 3.4-4.2GHz). To achieve high backoff efficiency, the Envelope-Tracking Power Amplifier (ET-PA) is one of the promising solutions, which lends itself more readily to operation over wide carrier frequency range than Doherty or Outphasing approaches.

At present, the Doherty Power Amplifier (DPA) is most often used in basestation PAs, instead of ET-PA. Efficiency of reported ET-PAs [1]-[4] is of order 10% less than that of DPAs [5],[6]. It is thus important to improve the efficiency of ET-PAs for the targeted base station frequency range.

In this work we report an ET-PA operating over a wide frequency range (3.6-4.0 GHz) which achieves record total efficiency of 47%, under LTE modulation (6.5dB PAPR). To achieve this result, our system uses 0.15um GaN FETs for both envelope amplifier and RF-PA, and incorporates several innovations: 1) soft-switching buck-converter (Soft-SWBC) within the Envelope Amplifier/Modulator (EA), to improve efficiency at high switching rates; and 2) optimized design of RF-PA to achieve both broad bandwidth and high power-added efficiency (PAE) over a wide range of drain supply voltages.

Soft-switching technique can reduce power loss of the buck-convertor (BC), by avoiding overlap of voltage and current waveforms during switching commutation [7]. The ET-PA achieved total efficiency of 39.5-46.7%, output power of 31.2-31.5dBm over 3.6-4.0GHz with 20MHz LTE signals. With DPD implemented in the DFE environment, adjacent channel leakage ratio (ACLR) was below -45dBc while maintaining 47% total efficiency at 3.6GHz. This, to the best of the authors' knowledge, is the highest efficiency yet reported for an ET-PA at this carrier frequency range.

II. Circuit Design and Measurement

A. Soft-Switching Envelope Amplifier/Modulator

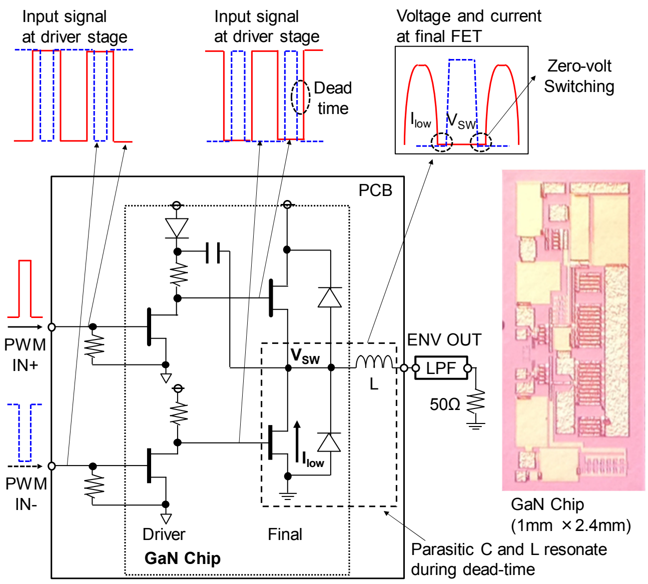

Fig. 1. Circuit diagram of the soft-switching buck-converter and chip photo.

Figure 1 shows the circuit diagram of the BC based on the soft-switching technique used in the EA, along with its chip photo. The circuit employs a boot-strap technique for the high-side driver, to improve the driver stage efficiency. The Soft-SWBC employs a diode and an inductor which resonates with output capacitance of the GaN FETs at the switching frequency. The input signal to the final stage was provided with an appropriate dead-time (no overlap between high and low side signals for a suitable time). As a result, at the switching transitions, overlap of voltage and current was avoided at the FET. On the other hand, the output signal was maintained by the resonance between the output capacitance of FET and inductor on the PCB board. Soft-switching operation reduces the energy loss during the output switching transitions, thus it minimizes the contribution to overall power loss which is proportional to switching frequency f_{sw}. It is therefore an enabler for efficient operation at higher switching frequencies, appropriate for wide modulation signals.

Figure 2 shows the switching frequency dependence of the Soft-SWBC and hard-switching BC (Hard-SWBC). In the Soft-SWBC case, the output inductor was optimized based on the switching frequency, along with the load and supply voltage of the drivers within the GaN chip. The Hard-SWBC did not have the resonant inductor and diodes. At 200MHz switching frequency, measured Soft-SWBC efficiency was 77% with 50Ω load for 6.5dB PAPR 20MHz modulation signal with 40% detroughing. Even with high switching frequency of 450MHz, it still maintained 67% total efficiency (> 20% higher efficiency compared with Hard-SWBC, as expected from reduced switching transition loss).

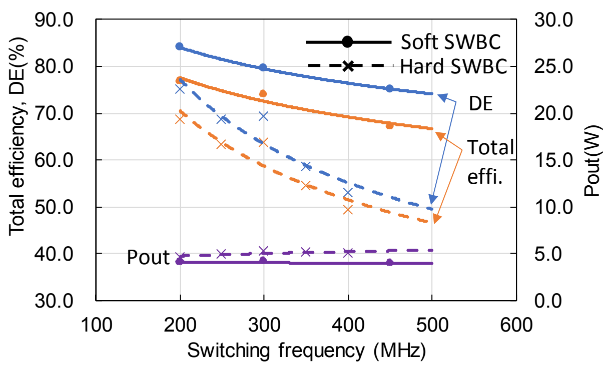

Fig. 2. Switching frequency dependence of the soft-switching and hard-switching buck-converter.

B. Wideband High Efficiency RF Power Amplifier

A photo and circuit diagram of the wideband RF-PA are shown in Fig. 3. The circuit was designed for wideband operation ranging from 3.4 to >4.0GHz. To maximize bandwidth, the real load impedance was designed to be 50Ω directly. Reactive load tuning used an output capacitance C_{ds} canceling inductor close to the GaN FET output. To achieve high efficiency for the targeted base station frequency range, a 2[nd] harmonic tuning circuit was employed. This circuit included a parallel combination of 90 degree open and short stubs at 2[nd] harmonic (which provides a short overall) placed at an appropriate electrical length from the GaN FET drain. At the fundamental frequency, these were 45 degree open and short stubs in parallel, which approximately cancel each other, and thus do not affect the fundamental frequency matching.

Figure 4 shows measured PAE vs. output power of the wideband RF-PA at 3.6GHz with various fixed power supply voltages from 10 to 30V (2.5V steps) with continuous wave signals. Even for low supply voltages, the RF-PA achieved PAE over 65%. Saturation output power is of order 39dBm at 30V.

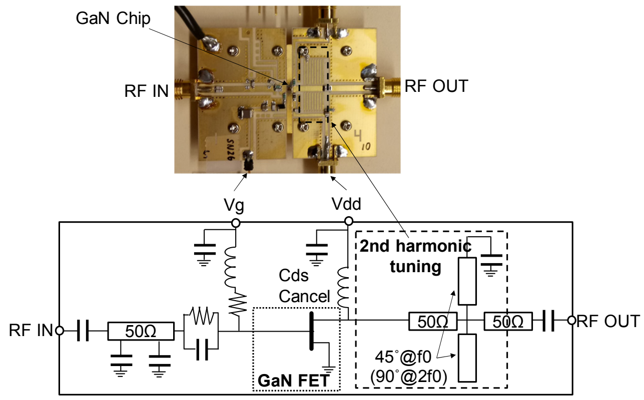

Fig. 3. Circuit diagram and photo of the RF-PA.

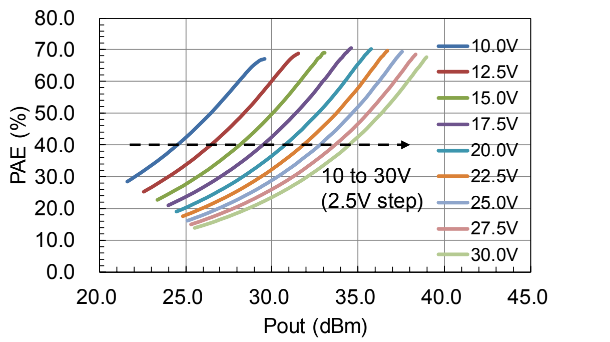

Fig. 4. Measured PAE vs. output power of RF-PA at 3.6GHz with various fixed power supply voltages.

III. ET-PA OPERATION AND MEASUREMENT

The measurement setup including DFE environment is described in Fig.5. The DFE is implemented in a single RF system-on-a-chip [8]. The ET-PA consists of the Soft-SWBC and the wideband RF-PA described above, and a low pass filter (LPF), which had a cut off frequency of 94MHz. The original baseband signal for 20MHz LTE was generated through Matlab in a remote computer and stored in the memory of the system. Based on the baseband signals, the input signals for the Soft-SWBC and RF-PA were generated. The binary input signal for the Soft-SWBC was generated with Pulse Width Modulation (PWM) using a switching frequency of 184.32MHz and a 11.8Gbps frequency to define the modulated pulse widths (oversampling ratio of 64).

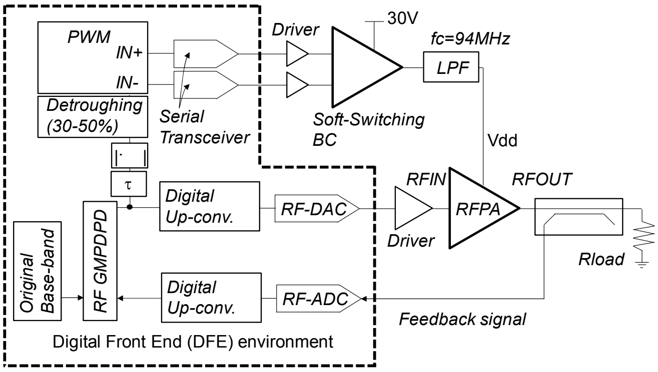

Fig. 5. ET measurement setup and signal generation algorithm.

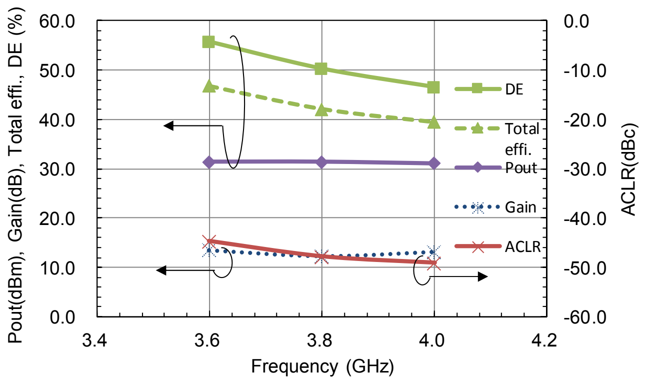

Fig. 6. Frequency dependency of ET-PA without DPD.

Before starting the measurement, the delay between the RF branch and envelope branch was measured and compensated by the delay adjuster block. The desired output waveform of Soft-SWBC was designed not to reach below approximately 10V, since peak efficiency at 10V decreased slightly in comparison with higher power supply voltages (Fig.4). Therefore, the generated envelope waveform was detroughed to approximately 40%. Also, the BC with boot-strap structure has a 95% upper limit for duty cycle. As a result, the PWM signal was designed to have a duty-cycle range of 40-95%. In addition, dead-time was added between high and low side input signals to achieve soft-switching operation. The dead-time was around 0.3ns for both the rising and falling signal edges.

An LTE signal with 20MHz bandwidth, 6.5dB PAPR was then applied, at carrier frequencies in the range 3.6-4.0GHz. As described in Fig. 5, output signals from the PA were captured by the overall system, and used to perform digital predistortion using the RF Generalized Memory-Polynomial DPD (RF-GMPDPD) approach. The distorted signals were also used to calculate binary input signals for the Soft-SWBC. This allowed us to perform the DPD, since signal generation, capture, predistortion, signal sampling and signal output were all done in the same system.

Figure 6 shows measured frequency dependency of ET-PA. Over 40% total efficiency was achieved across the measured frequency range with under -45dBc ACLR and 31.2-31.5dBm output power. Total efficiency includes power consumed by EA driver and final stages and RF-PA input power. Maximum total efficiency reached 47% at 3.6GHz. This, to the best of the authors' knowledge, is the highest efficiency yet reported for an ET-PA in this frequency range.

TABLE I compares ET operation with normal fixed voltage operation (obtained using fixed-duty cycle of 90% signal input to the BC with no dead-time, and switching frequency of 200MHz). ET operation boosted total efficiency by more than 10%, from ~ 31-34% to 42-47%.

TABLE II shows the state-of-the-art performance of ET-PAs and DPAs. Compared with other ET-PAs, the ET-PA reported here has the highest efficiency while meeting the 3GPP linearity requirement (ACLR < -45dBc) and total efficiency > 40% (highest efficiency = 47%) for a wideband range. The ET-PA efficiency is comparable to that achieved in DPAs, and the ET-PA RF frequency range is wider than that of DPAs with wide modulation signals [6].

TABLE I

COMPARISON OF FIXED DUTY AND ENVELOPE TRACK

Input Signal			Drain Supply	Measurement results			
Freq.	Mod. BW	PAPR		Pout	Gain	Total Effi.	ACLR1
(GHz)	(MHz)	(dB)		(dBm)	(dB)	(%)	(dBc)
3.4-4.0	20	6.5	Fixed Duty Cycle	32.0	14.1-15.7	30.8-33.9	-25.7- -27.8
3.4-4.0	20	6.5	Envelope track	32.0	12.5-14.1	42.2-47.4	-29.9- -32.2

TABLE II

STATE-OF-THE-ART PERFORMANCE OF WIDEBAND PAS

Ref.	Type	Input Signal			DPD	Measurement results			
		Freq.	Mod. BW	PAPR		Pout	Gain	Total Effi,	ACLR1
		(GHz)	(MHz)	(dB)		(dBm)	(dB)	(%)	(dBc)
[1]	ET-PA	0.5-1.75	5	6.6	w/ DPD	33-36	10.3-13.9	25-31	-47.5
[2]	ET-PA	0.9-2.15	80	6.5	w/ DPD	30-30.7	15.0-18.2	32.1-35.5	-45
[3]	ET-PA	1.84	75	10.4	w/ DPD	38.5	-	38.5	-45
[4]	ET-PA	1.80	120	10.0	w/ DPD	39	-	38.5	-46.5
[5]	DPA	3.0-3.6	CW	6.0	-	38.0	10.0	34.2-50.4	-
[6]	DPA	3.45-3.55	100	9.7	w/ DPD	34	10.5	51.0	-50
[Here]	ET-PA	3.6-4.0	20	6.5	w/ DPD	31.2-31.5	12.3-13.6	39.5-46.8	-44.5- -49.8

IV. CONCLUSION

These results show that the ET system implemented with GaN technology is a cutting-edge RF amplifier technology for next-generation base station applications, which can cover a broad carrier frequency range in the sub-6GHz region with high efficiency for the required high PAPR signals.

ACKNOWLEDGMENT

The authors would like to acknowledge contribution from NOKIA-Bell Labs, the UCSD Center for Wireless Communications and Mitsubishi Electric Corporation. The authors would like to thank Jarmo Marttila and Xilinx for providing the RFSoC hardware environment.

REFERENCES

[1] J.J. Yan *et al*., " Design of a 4-W Envelope Tracking Power Amplifier With More Than One Octave Carrier Bandwidth," *IEEE J. Solid-State Circuits, vol. 47, no. 10, pp. 2298–2308, Oct. 2008.*

[2] S. Sakata *et al.,* "An 80MHz Modulation Bandwidth High Efficiency Multi-band Envelope-Tracking Power Amplifier Using GaN Single-Phase Buck-Converter," *2017 IEEE MTT-S Int. Microw. Symp., Honolulu, HI.*

[3] N. Wolff *et al.,* "Highly Efficient Class-G Supply-Modulated Amplifier with 75 MHz Modulation Bandwidth for 1.8-1.9 GHz LTE FDD Applications," *2017 IEEE MTT-S Int. Microw. Symp., Honolulu, HI.*

[4] N. Wolff *et al.,* "Highly Efficient 1.8-GHz Amplifier with 120-MHz Class-G Supply Modulation," *IEEE Trans. Microw. Theory Techn., vol. 65, no. 12, pp. 5223-5230, December 2017.*

[5] J. M. Rubio *et al*., "3–3.6-GHz Wideband GaN Doherty Power Amplifier Exploiting Output Compensation Stages," *IEEE Trans. Microw. Theory Techn., vol. 60, no. 8, pp. 2543-2548, August 2012.*

[6] M. Özen, C. Fager, "Symmetrical Doherty Amplifier with High Efficiency over Large Output Power Dynamic Range," *2014 IEEE MTT-S International Microwave Symp., Tampa, FL.*

[7] D. Maksimovic, "Design of the zero-voltage-switching quasi-square-wave resonant switch," *1993 Power Electronics Specialists Conference, Seattle, WA*.

[8] B. Farley *et al*., "A Programmable RFSoC in 16nm FinFET Technology for Wideband Communications," *2017 IEEE Asian Solid-State Circuits Conference, Seoul, Korea*.